

# Photocatalyzed degradation of polymers in aqueous semiconductor suspensions

## V. Photomineralization of lactam ring-pendant polyvinylpyrrolidone at titania/water interfaces

Satoshi Horikoshi<sup>a</sup>, Hisao Hidaka<sup>a,\*</sup>, Nick Serpone<sup>b</sup>

<sup>a</sup> Frontier Research Center for the Global Environment Protection, Meisei University, 2-1-1 Hodokubo, Hino, Tokyo 191-8506, Japan

<sup>b</sup> Department of Chemistry and Biochemistry, Concordia University, 1455 de Maisonneuve Blvd. West, Montreal, Que., Canada H3G 1M8

Received 1 May 2000; received in revised form 31 July 2000; accepted 3 October 2000

### Abstract

The mechanism of photo-oxidation of the water-soluble polyvinylpyrrolidone (PVP) having a pendant five-membered lactam ring is complicated by the manner by which the macromolecule adsorbs on the TiO<sub>2</sub> particle surface in a heterogeneous dispersion. Experimental results and computer simulation of the initial process(es) infer three major steps for the photodegradation of the PVP structure. The first step is adsorption (or coagulation) of PVP on TiO<sub>2</sub> particles as evidenced by the size distribution of TiO<sub>2</sub> particles by dynamic light-scattering and by the electric charge on the TiO<sub>2</sub> particle surface assayed by  $\zeta$ -potential measurements. Molecular orbital simulations of initial processes were calculated at the AM1 level using the MOPAC system available in the CAChe package. The second step, namely attack of PVP by  $\bullet$ OH and/or  $\bullet$ OOH radicals, involves cleavage of the PVP main chain and opening of the lactam ring in the PVP structure probed by temporal UV spectral changes and by a decrease of the molecular weight using gel permeation chromatographic methods. Additional details of the photo-oxidation mode of the lactam ring was examined by a detailed examination of the photo-oxidation of the model compound 2-pyrrolidone to ascertain formation of  $\bullet$ OH radical adducts, opening of the lactam ring, and identification of intermediates by HPLC, and <sup>13</sup>C- and <sup>1</sup>H-NMR methods. The final major step in the mechanism involves generation and subsequent conversion of the primary amine (methylamine from opening of the lactam ring) to yield ultimately NH<sub>4</sub><sup>+</sup> and NO<sub>3</sub><sup>-</sup> ions, and conversion of the propanoic acid to acetic and formic acids and then to CO<sub>2</sub>. The effects of the extent of polymerization and variation in light intensity were examined using PVP samples having different hardness factors (hf) of 15 and 30, and different light intensities (namely, 1, 2, 3 and 4 mW cm<sup>-2</sup>), respectively. © 2001 Elsevier Science B.V. All rights reserved.

**Keywords:** Photo-oxidation; Photodegradation; Polyvinylpyrrolidone; 2-Pyrrolidone; Photocatalysis; Titanium dioxide

### 1. Introduction

Studies on photo-oxidation are typically carried out to examine the photodeterioration of various types of household relevant products. Techniques to treat such products have included combustion, pyrolysis, biodegradation with bacteria, supercritical water oxidation, microwave hydrolysis, chemical oxidation, and recycling. Treatment of domestic and industrial plastics presents an unusual challenge to society. Studies on polymeric materials have typically focused on preventing their degradation by physical and chemical methods, with the former implicating photodegradation with UV light, thermal and electric degradation. Chemical meth-

ods involve degradation by oxygen, ozone, water, steam, chemical oxidants and microorganisms. Polymeric materials are usually resistant or slow to degrade by these means. Consequently, their degradation has proven somewhat difficult to achieve. The photodegradation pathway of such plastics as polypropylene (PP), polystyrene (PS), polyethylene (PE), polyvinylchloride (PVC), and polyacrylate (PA) by UV light irradiation has recently been the object of some reports [1–8].

The photodecomposition of polymeric materials in suspensions containing the TiO<sub>2</sub> anatase pigment (but not by the rutile form) was reported nearly two decades ago [9,10]. The photodecomposition of water-soluble polymers (e.g., polyethyleneglycol, PEG) [11,12], solid polymers (e.g., PVC) [13,14] and biopolymers such as amino acids, DNA and RNA [15–20] was reported in more recent studies.

\* Corresponding author.

E-mail address: hidaka@epfc.meisei-u.ac.jp (H. Hidaka).

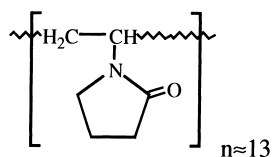
Various procedures to dispose of some of these polymeric materials have both beneficial and deleterious effects from the point of view of efficiency, economics and toxicity. In this regard, the photocatalytic degradation method causes no formation of toxic final products, as confirmed by Ames mutagenicity assays.

The mechanism(s) of the photomineralization of a polymeric structure is (are) often complex and unknown because of the uncertain extent of adsorption from the size ratio of polymer to TiO<sub>2</sub> particle, and from an overlap of photo-oxidation and formation of additional unidentified intermediates. The present study focuses on three aspects, namely (1) the photodegradation mechanism of a large structure such as the PVP polymer in a TiO<sub>2</sub>/H<sub>2</sub>O dispersion system, (2) the initial photo-oxidation process taking place on the TiO<sub>2</sub> surface, and (3) the photomineralization process involving the ring moiety in the polymeric material. The compound 2-pyrrolidone was used as a model of the pendant ring function in polyvinylpyrrolidone (PVP). Generally, PVP is used in cosmetics (hairsprays), in medicine (blood plasma extender) and in the construction industry (in plywood adhesives and sealing composites). Recently, the polymer has also been utilized in electrotechnics, electro-optics and in the production of selective membranes [21–24]. The facile photodegradation of a large quantity of PVP material would be significant environmentally and thus is worthy of being investigated in some details.

## 2. Experimental

### 2.1. Materials

Polyvinylpyrrolidone (PVP;  $-\text{[C}_6\text{H}_9\text{NO]}_n-$ , see structure below) having hardness factors (hf) of 15 and 30, and 2-pyrrolidone were supplied by Tokyo Kasei Co. Ltd. Titanium dioxide was Degussa P-25 (particle size, 20–30 nm by TEM observation; composition is 87% anatase and 13% rutile determined by X-ray diffraction; surface area, 53 m<sup>2</sup> g<sup>-1</sup> assessed by BET measurement).



### 2.2. Photodegradation procedures and analytical methods

Polyvinylpyrrolidone (10 mg) and TiO<sub>2</sub> particles (100 mg) in an aqueous dispersion (50 ml) were contained in a 124 ml Pyrex vessel. The dispersion was sonicated for ca. 5 min, purged with excess oxygen gas for 15 min, and then illuminated with a 75-W Hg-lamp (2.8 mW/cm<sup>2</sup>) under magnetic agitation. Subsequent to irradiation, the distribution of molecular weight in the PVP solution (after removal

of TiO<sub>2</sub>) was assayed by gel permeation chromatography (GPC) using an Asahipak GF-510 HQ column and a JASCO liquid chromatograph equipped with a refractive index (RI) detector; pure water was the eluent. Changes in the distribution of TiO<sub>2</sub> particle sizes were analyzed by dynamic light scattering (DLS) with a DLS/SLS-5000 system equipped with single photon detection [12]. The temporal change of  $\zeta$ -potential upon irradiation was measured with an Otsuka electrophoretic light scattering equipment. Cleavage of the lactam ring was analyzed with a JASCO UVDEC 660 spectrophotometer. The primary amine function was quantitatively determined by the fluorescamine method (0.03% (v/v) in acetone; borate buffer, pH = 9.0) using a JASCO FP-770 fluorophotometer [25,26]. The concentration of ammonium and nitrate ions was assayed by an ion chromatographic method employing a JASCO liquid chromatograph (HPLC) equipped with a CD-5 conductivity detector and either a Y-521 cation column or an I-524 anion column. The temporal evolution of CO<sub>2</sub> was monitored by gas chromatography with an Ookura Riken chromatograph (model 802; TCD detection) and a Porapack Q (CO<sub>2</sub> gas) column with helium as the carrier gas. The <sup>13</sup>C- and <sup>1</sup>H-NMR spectral profiles of the PVP structure (1 mg) in D<sub>2</sub>O solvent (5 ml) or of 2-pyrrolidone solutions (0.1 mM in D<sub>2</sub>O) were monitored after various illumination periods of TiO<sub>2</sub> (10 mg) dispersions using a JEOL 500 MHz FT-NMR spectrometer. The scanning times to obtain suitable <sup>13</sup>C-NMR and <sup>1</sup>H-NMR spectra were 1000 and 16 times, respectively. The concentration of carboxylic acids was determined with a JASCO liquid chromatograph (HPLC) using UV detection (wavelength = 191 nm) and a RSpak KC-811 column; the eluent was a HClO<sub>4</sub> solution (0.003%, v/v). A bromthymol blue solution (0.2 mM), also containing Na<sub>2</sub>HPO<sub>4</sub> (8 mM) and NaOH (2 mM), was employed as the indicator to assess the quantity of carboxylic acids. The photomineralization yield (%) was calculated on the basis of the expected percent mineralization yield for a 10 mg sample with unit molecular weight of {C<sub>6</sub>H<sub>9</sub>NO} (mol. wt. = 340).

Semi-empirical molecular orbital (MO) calculations of the frontier electron density of atoms toward radicals and of point charges on the 2-pyrrolidone atoms were carried out at the single determinant (Hartree–Fock) level with the optimal conformation having minimum energy obtained at the AM1 level. Calculations were performed with MOPAC 97 using the CAChe package implemented on a Windows system. UV absorption spectra of potential initial intermediate species were simulated using the ZINDO version 6.3 system also available in the CAChe package [20,27,28].

## 3. Results and discussion

The temporal changes in molecular weight (loss) occurring during the photodecomposition of PVP (hf = 15) and monitored by gel permeation chromatography (GPC) are illustrated in Fig. 1. Standard polyethyleneglycol samples

with molecular weights of 200, 400, 600, 1000, 2000 and 50,000 were used to calculate the molecular weights of PVP degradation products by this GPC technique. Before illumination (time = 0), the GPC patterns of polyvinylpyrrolidone showed molecular weight distributions of 18,641 (retention times,  $rt = 18$  min) and 1437 ( $rt \approx 25$  min); the peak at ca. 100 is due to some adventitious impurity. After 0.5 h of UV illumination, the PVP chain was shortened to fragments having molecular weights of 13,133, 6,859, and 1,179. Continued irradiation led to further fragmentation of PVP. Cleavage of the PVP chain after 4 h of irradiation caused the disappearance of the major peak at 1437 and a decrease of the other peaks to other molecular weight distributions at 1,934 and 308. Further irradiation led to additional diminution and to a substantial drop in the molecular weight distribution (see, e.g., the peak at  $rt \approx 20$  min) from 18,641 to 7,247.

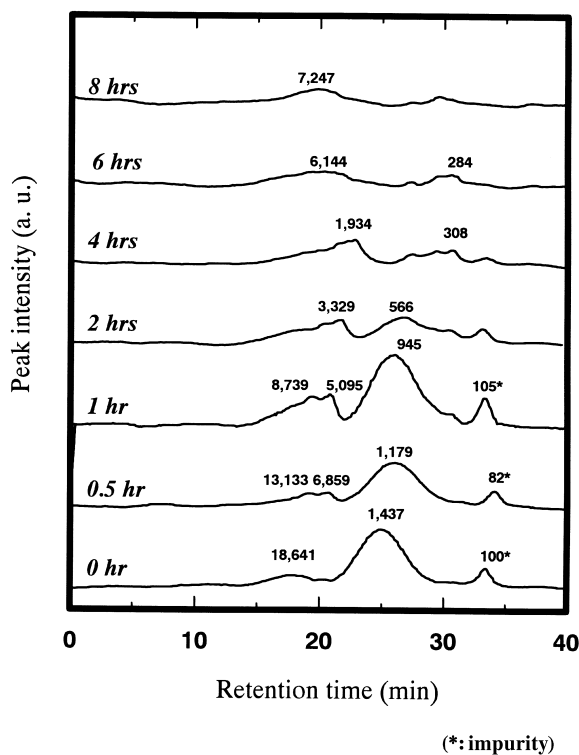
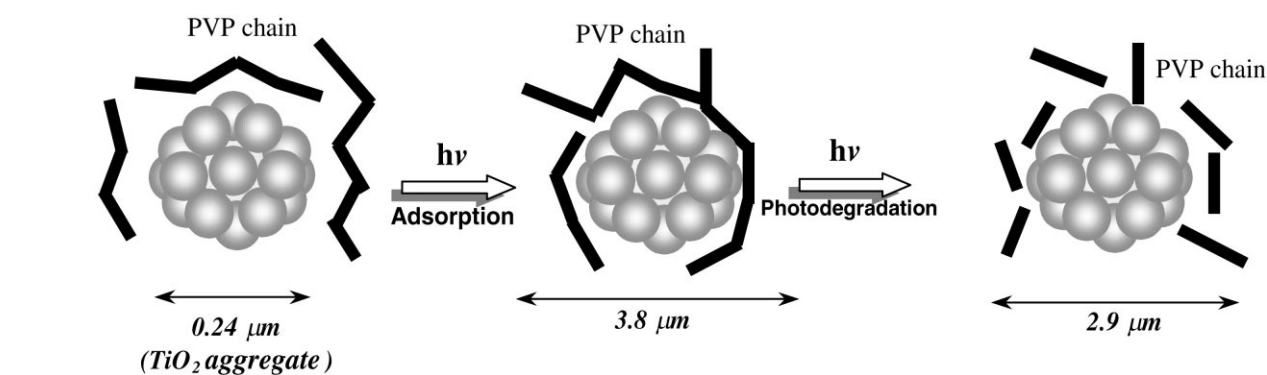


Fig. 1. Temporal gel permeation chromatographic profiles in the photodegradation of PVP ( $hf = 15$ ) under UV illumination with a Hg-lamp.

Dynamic light-scattering was employed to measure the aggregate size distribution of the  $\text{TiO}_2$  particles and aggregated assemblies in the  $\text{TiO}_2/\text{PVP}$  system (Fig. 2). The average diameter of the  $\text{TiO}_2$  aggregated particles was about  $0.24 \mu\text{m}$ . Transmission electron microscopy (TEM) images of  $\text{TiO}_2$  particles exhibited primitive crystallite sizes of about  $0.02\text{--}0.03 \mu\text{m}$  (diameter). Size distribution of aqueous PVP solutions ( $40 \text{ mg}/50 \text{ ml}$ ) exhibited a broad size range from a major distribution centered at ca.  $0.21 \mu\text{m}$  and a smaller one at  $50.8 \mu\text{m}$ . Addition of PVP chains to the  $\text{TiO}_2$  dispersion in the dark caused formation of larger  $\text{TiO}_2$  particle aggregates (ca.  $0.16$  and  $0.90 \mu\text{m}$ , dark conditions). On UV illumination, the  $\text{TiO}_2$  particle/PVP assembly decreased from an initial  $3.81 \mu\text{m}$  at  $0.25 \text{ h}$  to  $2.86 \mu\text{m}$  after  $8 \text{ h}$  owing to photo-oxidative cleavage of the PVP molecular chain.

Evidently, PVP is initially photoadsorbed on the surface of the  $\text{TiO}_2$  particle aggregates (illustrated above) which on irradiation leads to smaller fragments also adsorbed on  $\text{TiO}_2$ . The aggregation of  $\text{TiO}_2$  particles was accelerated by the photodegradation of PVP.

The temporal changes in the  $\zeta$ -potential and in pH during the photodegradation of PVP are reported in Fig. 3. The  $\zeta$ -potential and the pH of the PVP/ $\text{TiO}_2$  dispersion in the dark was  $14 \text{ mV}$  and  $4.8$ , respectively. On irradiation the  $\zeta$ -potential first dropped down to ca.  $3 \text{ mV}$  after  $3 \text{ h}$  and then increased to about  $16 \text{ mV}$  after  $7\text{--}8 \text{ h}$  of UV illumination. The pH decreased to about  $4.2$  after  $1 \text{ h}$  illumination and then increased to  $\sim 6.0$  after  $7\text{--}8 \text{ h}$ . The decrease of the  $\zeta$ -potential after the  $2\text{-h}$  irradiation period is due to the increase of pH as the pH approached the isoelectric point ( $pI = 6.3$ ) of  $\text{TiO}_2$ . After that, the  $\zeta$ -potential at the  $\text{TiO}_2/\text{water}$  interface remains low for ca.  $2 \text{ h}$ . At longer UV irradiation times (more than  $5 \text{ h}$ ), the  $\zeta$ -potential again increases probably caused by formation of intermediate cationic compounds. That is, the subsequent increase of the  $\zeta$ -potential is consistent with photocleavage of PVP on the  $\text{TiO}_2$  surface to yield smaller fragments during the course of the photodegradation of this polymer. Note also that as the pH of the photodegraded solution approaches the isoelectric point of  $\text{TiO}_2$  particles, the net charge of the  $\text{TiO}_2$  surface is neutral, thus facilitating aggregation of the  $\text{TiO}_2$  particles.

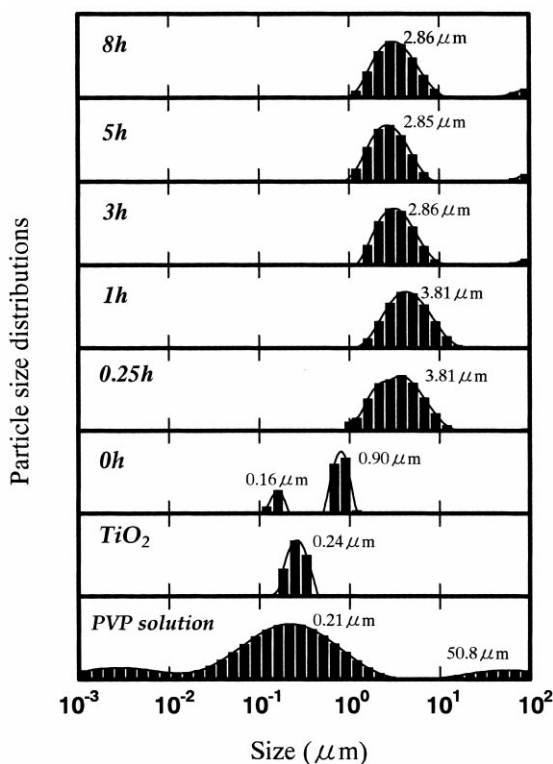


Fig. 2. Particle size distribution in the photodegradation of PVP ( $hf = 15$ ) in a  $TiO_2$  dispersion under UV exposure for 0, 0.25, 0.5, 1, 3, and 8 h. The PVP aqueous solution containing  $TiO_2$  particles was dispersed by sonication for 10 min.

The temporal evolution of  $CO_2$  gas in the photo-oxidative degradation of PVP is depicted in Fig. 4a. The effect of the degree of polymerization was examined for the two PVP samples with a hardness factor of 15 and 30 in a  $TiO_2$  (100 mg) aqueous dispersion (50 ml). Differences in the rate of generation of  $CO_2$  gas are somewhat negligible and hence independent of the hardness factor. In both instances, photomineralization yields of  $CO_2$  gas of ca. 50% were obtained for PVP after 8 h of irradiation. No further  $CO_2$  evolution

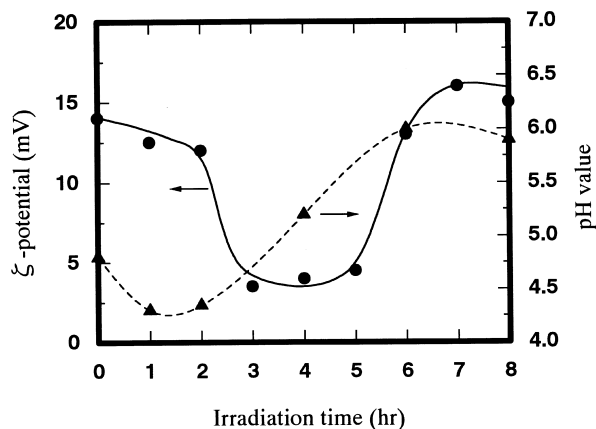


Fig. 3. Temporal  $\zeta$ -potential and pH changes in the photodegradation of PVP ( $hf = 15$ ). The aqueous dispersion (50 ml) containing  $TiO_2$  particles (100 mg) and PVP (10 mg) was diluted with water 400 times.

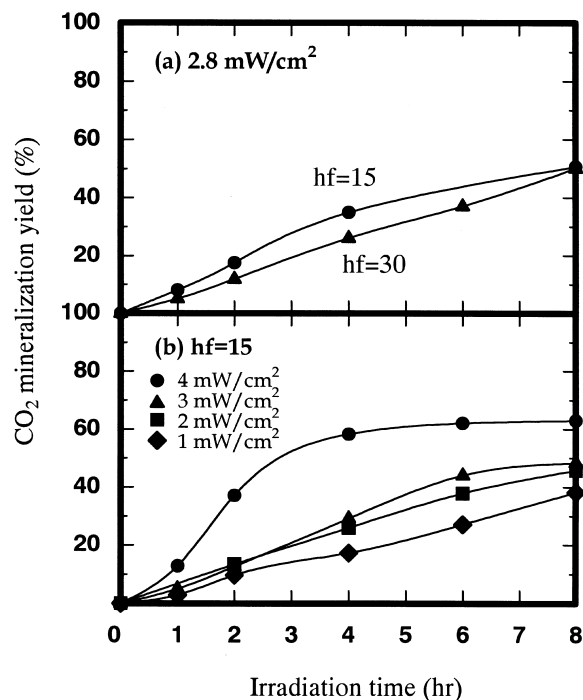


Fig. 4. (a)  $CO_2$  evolution in the photodegradation of PVP as a function of the hardness factor for  $hf = 15$  and  $hf = 30$ . (b) Effect of light intensity on the photodecomposition of PVP in a  $TiO_2$  dispersion system.

was seen from PVP degradation even after a 20-day illumination period. The effect of light intensity on the photomineralization of PVP is illustrated in Fig. 4b. Light intensity influences the degradation rate and the photomineralization yield significantly; e.g., as light intensity changed from 4, 3, 2 and  $1 \text{ mW cm}^{-2}$ , the  $CO_2$  mineralization yield decreased from 63%, to 50%, 45% and 38%, respectively, after an 8-h illumination period.

Evidence for ring opening of the lactam function in PVP is displayed in Fig. 5a. The attenuation maximum at ca. 230 nm in the UV absorption spectrum for the initial PVP/ $TiO_2$  dispersion first increased slightly on irradiation for ca. 2–3 h and then was significantly attenuated on further illumination to ca. 30% after 14 h. Formation of a primary amine was maximal after an irradiation period of about 5 h (see Fig. 5b), and subsequently degraded slowly being converted ultimately to  $NH_4^+$  and  $NO_3^-$  ions (see Fig. 5c and the inset to Fig. 5c). The formation yield of  $NH_4^+$  ions was 24%, whereas the yield of  $NO_3^-$  ions was 0% even after 14 h of illumination; the yields reached 64 and 15%, respectively, after 7 days. Further illumination for 15 days caused a drop in the yield of  $NH_4^+$  ions (38%) and a rise in the yield of  $NO_3^-$  ions (28%). This is understandable as  $NH_3$  is oxidized to  $NO_3^-$  ions in the presence of  $TiO_2$  particulates.

### 3.1. Photodegradation of 2-pyrrolidone

To obtain information on how the photodegradation of the pendant lactam ring moiety in the PVP structure takes place,

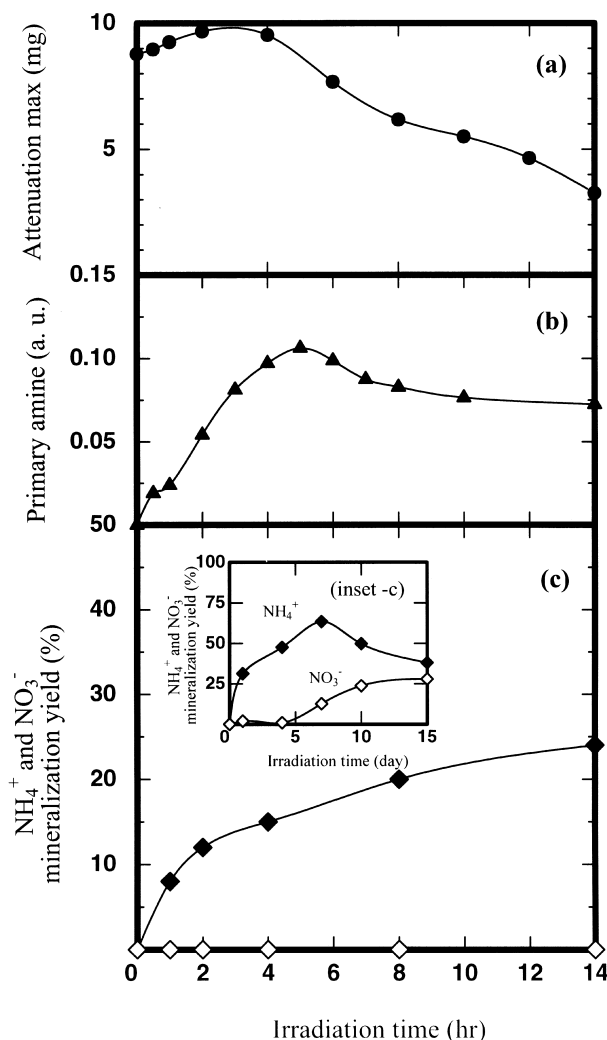


Fig. 5. (a) Relative UV spectral changes during the photo-oxidation of PVP ( $h\nu = 15$ ) in  $\text{TiO}_2$  dispersions under UV illumination. (b) Formation and disappearance of the primary amine during the photodegradation of PVP monitored by florescamine analysis. (c) Formation of  $\text{NH}_4^+$  and  $\text{NO}_3^-$  ions in the photodecomposition of PVP in  $\text{TiO}_2$  dispersions (100 mg/50 ml) under UV illumination; the inset depicts this formation for longer irradiation periods (days).

we examined the photodecomposition of 2-pyrrolidone ( $\text{HN}(\text{CH}_2)_3\text{CO}$ ). Opening of the 2-pyrrolidone ring was monitored by UV absorption spectroscopy, the results of which are displayed in Fig. 6. The 2-pyrrolidone (0.1 mM solution) exhibited a single band around 193 nm (abs. = 0.10) which shifted negligibly to 194 nm (abs. = 0.12) in the 2-pyrrolidone/ $\text{TiO}_2$  dispersion system prior to irradiation. UV illumination caused the absorption band to increase in intensity (abs. = 0.168) after 0.5 h concomitant with a further, albeit slight shift to 196 nm. On further irradiation, the band intensity decreased and the band position shifted to a lower wavelength. The negligibly small but nonetheless finite red shift of the UV absorption band to higher wavelengths is likely due to the effects of  $\bullet\text{OH}$  radicals on the  $\text{TiO}_2$  surface to produce hydroxylated intermediate species.

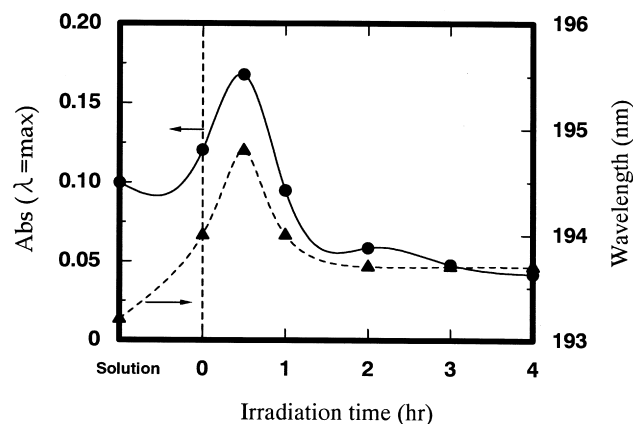


Fig. 6. UV spectral changes in band position and absorption intensity indicating opening of the 2-pyrrolidone ring.

Simulation of UV absorption for  $\bullet\text{OH}$  radical adducts was carried out using the ZINDO system available in the CACHE package. Table 1 summarizes the formation of the various hydroxylated intermediate species and the corresponding changes in the maximum peak positions in the UV absorption spectrum. ZINDO calculations are useful in inferring some of the initial steps in the photodegradation pathway of 2-pyrrolidone from a comparison of the calculated expectations with the experimental results.

Table 1

Calculation of the UV absorption bands for various species of the 2-pyrrolidone system using the ZINDO component in the CACHE package

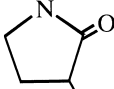
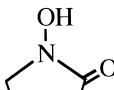
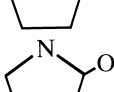
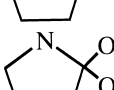
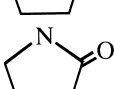
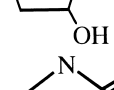
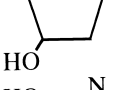
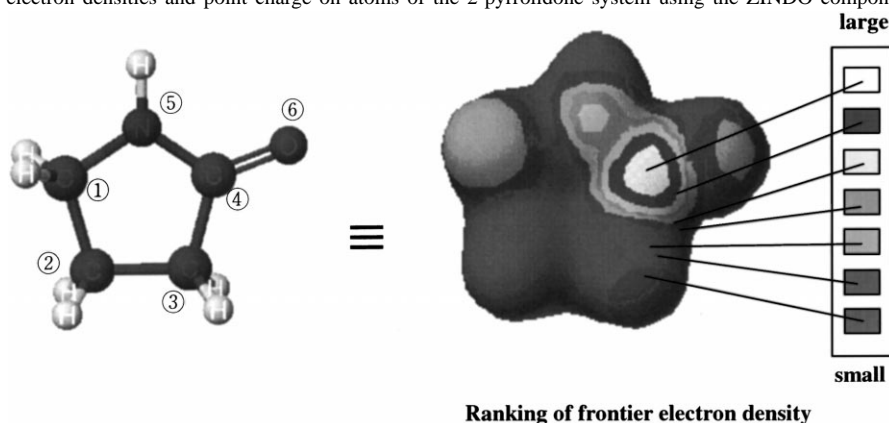
	198 nm
	203 nm
	No UV absorption
	No UV absorption
	195 nm
	195 nm
	193 nm

Table 2

Calculation of formation electron densities and point charge on atoms of the 2-pyrrolidone system using the ZINDO component in the CAChe package



Atom	Frontier electron density	Point charge
C <sup>1</sup>	0.40481	-0.0481
C <sup>2</sup>	0.41866	-0.1866
C <sup>3</sup>	0.41970	-0.1970
C <sup>4</sup>	0.36529	0.3471
N <sup>5</sup>	0.53572 <sup>a</sup>	-0.3572 <sup>a</sup>
O <sup>6</sup>	0.65816 <sup>a</sup>	-0.5816 <sup>a</sup>
H <sup>7</sup>	0.08870	0.1123
H <sup>8</sup>	0.08880	0.1114
H <sup>9</sup>	0.08864	0.1136
H <sup>10</sup>	0.08864	0.1136
H <sup>11</sup>	0.08581	0.1419
H <sup>12</sup>	0.08565	0.1435
H <sup>13</sup>	0.07128	0.2872

<sup>a</sup> See text for explanation.

UV absorption by 2-pyrrolidone is expected to change with addition of  $\bullet\text{OH}$  radicals to the 2-pyrrolidone ring. We therefore presume that the UV spectral increase in band intensity and changes in band positions seen in Fig. 6 occur because of addition of  $\bullet\text{OH}$  radicals to the nitrogen heteroatom and carbon atoms, as expected from the calculated frontier electron densities and negative point charges in the 2-pyrrolidone atoms. Table 2 shows that the N<sup>1</sup> and O<sup>6</sup> atoms bear the richest frontier electron densities in the 2-pyrrolidone ring, and consequently are poised to interact strongly with the electrophilic  $\bullet\text{OH}$  radicals. Moreover, the relatively large negative point charges on the O<sup>6</sup> and N<sup>1</sup> atoms would lead the ring structure to adsorb onto the positively charged TiO<sub>2</sub> surface through the N–C=O function. Of consequence, the latter would likely be the prime target for  $\bullet\text{OH}$  radical attack.

The temporal <sup>13</sup>C-NMR spectral patterns during the photo-oxidation of 2-pyrrolidone in a D<sub>2</sub>O solution (0.1 mM) are illustrated in Fig. 7. The initial pattern of four peaks is unchanged after 0.5 h of UV illumination, except for an additional new peak appearing at 32.19 ppm, which increased upon further irradiation. By contrast, the original four peaks of 2-pyrrolidone decreased in magnitude. The nature of this new peak was probed by <sup>1</sup>H-NMR spectral identification using a 2-pyrrolidone/D<sub>2</sub>O solution. Under these conditions, after 15 min of UV irradiation a

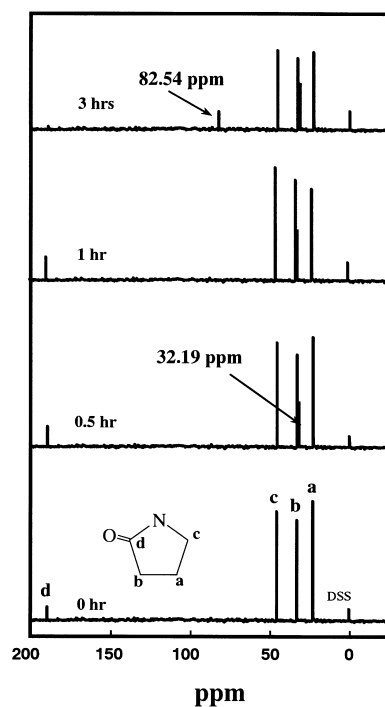
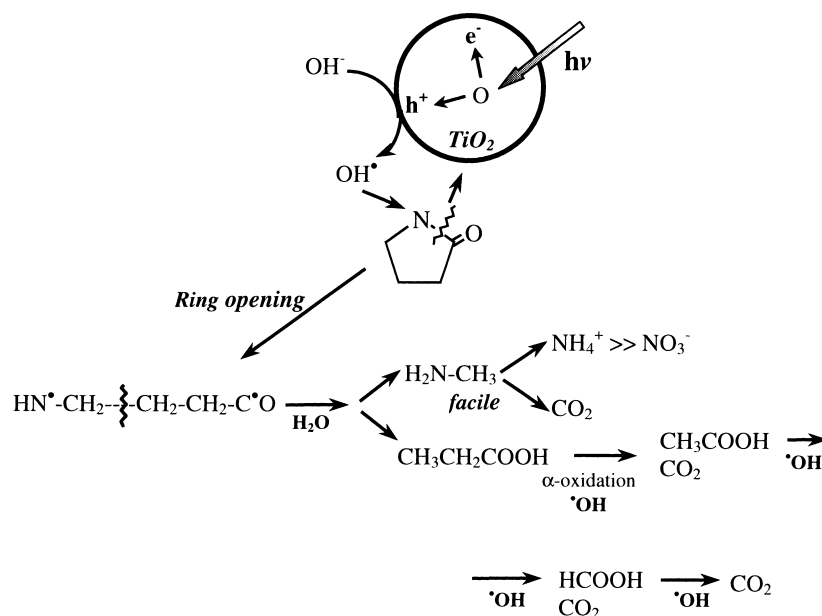


Fig. 7. Temporal changes in the <sup>13</sup>C-NMR spectral patterns during the photo-oxidation of 2-pyrrolidone in D<sub>2</sub>O solvent (0.1 mM, 10 ml) in a TiO<sub>2</sub> (10 mg) dispersion system.

new NMR singlet peak was seen at 2.79 ppm (vs TMS). Both the  $^{13}\text{C}$ - and the  $^1\text{H}$ -NMR spectral peaks at 32.19 and 2.79 ppm, respectively, are consistent with the presence of methylamine, a  $\text{D}_2\text{O}$  solution of which displays a  $^{13}\text{C}$ -NMR peak at 30 ppm ( $\text{C}^*\text{H}_3\text{NH}_2$ ) and a  $^1\text{H}$ -NMR singlet peak ( $\text{CH}_3^*\text{NH}_2$ ) at 2.5 ppm. Indeed, the initial photodegradation of 2-pyrrolidone yields methylamine and propanoic acid;

pathway for the model compound 2-pyrrolidone. The first step is the approach of the carbonyl function onto the positively charged surface of the  $\text{TiO}_2$  particles. Subsequently, with the high frontier electron densities of the  $\text{N}^1\text{-C}^2=\text{O}^6$  portion, we infer that  $\cdot\text{OH}$  radicals attack and cleave the  $\text{N}^1\text{-C}^2$  bond. The active  $\text{HN}^\bullet\text{-(CH}_2\text{)}_3\text{-C}^\bullet\text{O}$  radical is further cleaved at the  $\beta\text{-}\gamma$  carbon-carbon bond leading to the formation of methylamine and propanoic acid.



the latter was identified by HPLC techniques. Subsequently, the propanoic acid is photo-oxidized to acetic and formic acids as also confirmed by HPLC analyses.

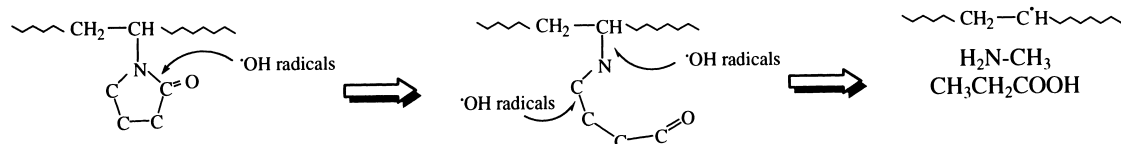
The temporal evolution of  $\text{CO}_2$  gas and formation of  $\text{NH}_4^+$  and  $\text{NO}_3^-$  ions in the photodecomposition of 2-pyrrolidone are depicted in Fig. 8. Evolution of  $\text{CO}_2$  occurred in two stages; one stage took place in less than 4 h of irradiation, while the second stage occurred beyond the 4-h period to reach 65% of the expected mineralization yield after 8 h of illumination. For the same period, photodecomposition of 2-pyrrolidone yields 82% of the expected amount of  $\text{NH}_4^+$  ions and ca. 8.5% of  $\text{NO}_3^-$  ions. Total conversion of the nitrogen atom to 91% yield appears to be more effective than mineralization of the carbon atoms to  $\text{CO}_2$  gas. Evolution of  $\text{CO}_2$  in the first stage and efficient formation of  $\text{NH}_4^+$  ions originate from the photo-oxidation of the methylamine intermediate. The second stage of  $\text{CO}_2$  gas formation occurs by  $\alpha$ -oxidation of the propanoic, acetic and formic acid intermediates.

### 3.2. Photomineralization pathway of 2-pyrrolidone

On the basis of the above results, it is now possible to infer and summarize some of the details of the photodegradation

Then there occurs rapid degradation of methylamine to produce  $\text{NH}_4^+$  ions and  $\text{CO}_2$  gas which comprises 25% of the total carbon atoms in 2-pyrrolidone. Continued photodegradation of propanoic acid to acetic and formic acids via  $\alpha$ -oxidation occurs more slowly than that of methylamine (see scheme). Note that the formation of methylamine was also detected in the initial photo-oxidation of PVP in  $\text{TiO}_2$  aqueous dispersion systems by  $^{13}\text{C}$ - and  $^1\text{H}$ -NMR techniques. Thus, photodecomposition of the model compound 2-pyrrolidone provides clues for the photodegradation mechanism of the side lactam ring in the PVP structure.

The photodegradation of PVP under strong UV light illumination was also reported recently by Kaczmarek et al. [29]. These authors inferred oxidation of the main chain in the PVP structure and cleavage of the side lactam ring from the main chain. Our present results indicate that photodecomposition of PVP in  $\text{TiO}_2$  aqueous dispersions is first preceded by saturation adsorption of PVP onto the  $\text{TiO}_2$  particulates through the  $\text{N-C=O}$  function of the pendant lactam ring. The progress of the photo-oxidative reaction is relatively slow, and occurs first by an opening of the lactam ring moiety and subsequent formation of the primary amine (methylamine; by NMR spectra for photo-oxidation of PVP) and propanoic acid as initial intermediates (illustrated below).



No photo-oxidation of the intermediates occurred under UV illumination for a few days owing to adsorption of the PVP main chain on the  $\text{TiO}_2$  aggregate that covered the surface active sites. The final process was photomineralization to  $\text{NH}_4^+$  ions and  $\text{CO}_2$  gas; however, the relevant reactions were rather slow (compare results in Fig. 5c and 8).

#### 4. Concluding remarks

The frontier electron densities calculated using the MOPAC system for  $\bullet\text{OH}$  radical attack on PVP suggest the nature of the first process of photocleavage. The frontier electron densities on nitrogen and oxygen atoms in the PVP structure ( $n \approx 13$  units) are, respectively, 1.2 times and 1.3 times those of the carbon atoms. We inferred then that the initial step is adsorption of PVP to the  $\text{TiO}_2$  particle surface followed by  $\bullet\text{OH}$  radical attack and cleavage of the single bond in the  $\text{N}-\text{C}=\text{O}$  function of the lactam moiety. This is followed by further  $\bullet\text{OH}$  attack to completely remove any remnant groups of the lactam ring in the PVP structure.

Contrary to an earlier report, the photo-oxidative breakup of the pendant lactam ring is perhaps the most important feature in the photodecomposition of the PVP structure. We propose that opening of the lactam ring is the initial step with the formation of a primary amine and propanoic acid, followed by formation of  $\text{NH}_4^+$  and  $\text{NO}_3^-$  ions in the ultimate final step, together with  $\text{CO}_2$ .

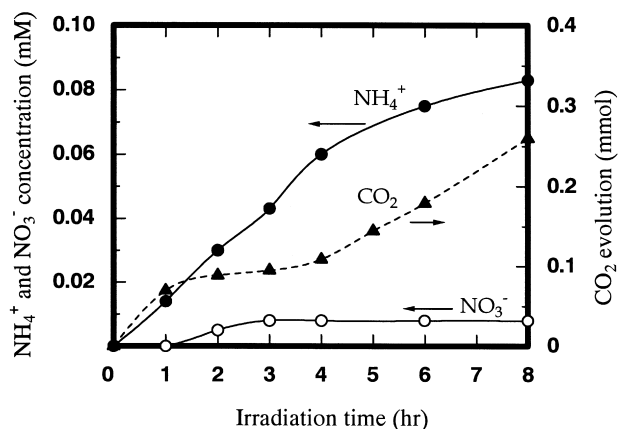


Fig. 8. Evolution of  $\text{CO}_2$  gas and formation of  $\text{NH}_4^+$  and  $\text{NO}_3^-$  ions in the photodecomposition of 2-pyrrolidone (0.1 mM) in a  $\text{TiO}_2$  dispersion (100 mg/50 ml) system under UV illumination.

#### Acknowledgements

This research was supported by a Grant-in-Aid for Scientific Research from the Ministry of Education, Science, Sports, and Culture of Japan (No. 10640569) and by Frontier Research Promotion Project Foundation (to HH). The work in Montreal is gratefully sponsored by the Natural Sciences and Engineering Research Council of Canada (to NS). The authors also wish to thank N. Watanabe, T. Kakuta and N. Shimizu for their technical assistance.

#### References

- [1] C. Decker, K. Zahouily, *Polym. Degrad. Stab.* 64 (1999) 293.
- [2] C. Decker, K. Zahouily, *J. Polym. Sci. A* 36 (1998) 2571.
- [3] J.W. Martin, J.W. Chin, W.E. Byrd, E. Embree, K.M. Kraft, *Polym. Degrad. Stab.* 63 (1999) 297.
- [4] M.S. Rabello, J.R. White, *Polym. Degrad. Stab.* 56 (1997) 55.
- [5] M.S. Rabello, J.R. White, *Plastics Rubber and Composites Process and Applications* 25 (1996) 237.
- [6] H. Kaczmarek, *Eur. Polym. J.* 12 (1995) 1175.
- [7] Li Tong, J.R. White, *Polym. Degrad. Stab.* 53 (1996) 381.
- [8] S. Denizligil, W. Schnabel, *Angew. Makromol. Chem.* 229 (1995) 73.
- [9] G. Irick Jr., G.C. Newland, R.H.S. Wang, *ACS Symp. Ser.* 151 (1981) 147.
- [10] H.G. Volz, G. Kaempf, H.G. Fitzky, A. Klaeren, *ACS Symp. Ser.* 151 (1981) 163.
- [11] S. Horikoshi, H. Hidaka, *J. Jpn. Soc. Color Mater. (Shikizai)* 71 (1998) 176.
- [12] S. Horikoshi, M. Ohta, H. Hidaka, J. Zhao, N. Serpone, *Recent Res. Develop. Polym. Sci.* 1 (1997) 149.
- [13] H. Hidaka, Y. Suzuki, K. Nohara, S. Horikoshi, E. Pelizzetti, N. Serpone, *J. Polym. Sci. A* 34 (1996) 1311.
- [14] S. Horikoshi, H. Hidaka, Y. Hisamatsu, N. Serpone, *Environ. Sci. Technol.* 32 (1998) 4010.
- [15] H. Hidaka, T. Shimura, K. Ajisaka, S. Horikoshi, J. Zhao, N. Serpone, *J. Photochem. Photobiol. A* 109 (1997) 165.
- [16] H. Hidaka, S. Horikoshi, K. Ajisaka, J. Zhao, N. Serpone, *J. Photochem. Photobiol. A* 108 (1997) 197.
- [17] R. Dunford, A. Salinaro, L. Cai, N. Serpone, S. Horikoshi, H. Hidaka, *J. Knowland, FEBS Lett.* 418 (1997) 87.
- [18] H. Hidaka, S. Horikoshi, N. Serpone, J. Knowland, *J. Photochem. Photobiol. A* 111 (1997) 205.
- [19] S. Horikoshi, N. Serpone, J. Zhao, H. Hidaka, *J. Photochem. Photobiol. A* 118 (1998) 123.
- [20] S. Horikoshi, N. Serpone, S. Yoshizawa, J. Knowland, H. Hidaka, *J. Photochem. Photobiol. A* 120 (1998) 63.
- [21] T. Tjarnhage, B. Skarman, B. Lindholmsethson, M. Sharp, *Electrochim. Acta* 41 (1996) 367.
- [22] D.M. Kelly, D.J.G. Vos, *Electrochim. Acta* 41 (1996) 1825.



- [23] J.R. Hwang, M.V. Sefton, *J. Membr. Sci.* 125 (1995) 257.
- [24] C. Vauclair, H. Tarjus, P. Schaelzel, *J. Membr. Sci.* 125 (1995) 293.
- [25] J.V. Castell, M. Cervera, R. Marco, *Anal. Biochem.* 99 (1979) 379.
- [26] M. Weigele, S.L. DeBernardo, J.P. Teng, W. Leimgruber, *J. Am. Chem. Soc.* 94 (1993) 1646.
- [27] K. Fukui, T. Yonezawa, C. Nagata, H. Shingu, *J. Chem. Phys.* 11 (1953) 1433.
- [28] S.D. Kahn, C.F. Pau, L.E. Overman, W.J. Hehre, *J. Am. Chem. Soc.* 108 (1986) 7381.
- [29] H. Kaczmarek, A. Kamińska, M. Świątek, J.F. Rabek, *Die Angew. Makromol. Chem.* 261 (1998) 109.